



Variability in Meropenem Distribution and Clearance in Children with Sepsis: Population-Based Pharmacokinetics with Assessment of Renal Biomarkers

Jennifer Le¹ · Julie Huynh¹ · Brandon Vo² · Annie Mai¹ · Robert H. Mak³ · Jeremiah D. Momper¹ · Edmund V. Capparelli^{1,3} · Helen Harvey⁴ · Sean Avedissian⁵ · Erin Bradley⁴ · Amy Sitapati^{3,6} · Karandeep Singh⁷ · John S. Bradley^{3,4}

Accepted: 2 March 2025 / Published online: 24 April 2025
© The Author(s) 2025

Abstract

Background and Objective Meropenem dosing to achieve therapeutic exposure in critically ill children with sepsis is challenging due to a spectrum of renal function, from augmented renal clearance (ARC) to acute kidney injury (AKI). The objective of this study was to define meropenem plasma concentrations and pharmacodynamic exposure metrics in children with septic shock during the first 3 days of PICU hospitalization.

Methods We prospectively evaluated meropenem clearance (CL_{MERO}) and volume of distribution ($V_{1-\text{MERO}}$), innovatively assessing renal biomarkers (serum creatinine [SCr], serum cystatin C [SCys], and neutrophil gelatinase-associated lipocalin [SNgal]), in infants aged ≥ 4 weeks and children on intravenous (IV) meropenem 20 mg/kg every 8 h from 2019 to 2023. Cases with sepsis were matched to controls without sepsis.

Results Analysis included 27 participants (19 cases and 8 controls) with 309 meropenem serum concentrations. Median age was 11.8 (range 0.6–19.6) years, weight 36.3 (7.2–98.0) kg, SCr 0.33 (0.09–2.57) mg/dL, SCys 451.1 (178.3–1824.1) ng/mL, and SNgal 180.7 (23.2–1403.0) ng/mL. A 2-compartment, population pharmacokinetic (PK) model via NONMEM best described data, with weight on V_{MERO} and allometric scaling on CL_{MERO} . Using the final model with SCys in $V_{1-\text{MERO}}$ and estimated glomerular filtration rate (eGFR)-MS in CL_{MERO} , the median $V_{1-\text{MERO}}$ was 0.23 (range 0.07–0.57) L/kg and CL_{MERO} 0.15 (0.05–0.49) L/h/kg, with eGFR-MS 139 (23–365) mL/min/1.73 m² from AKI to ARC. Meropenem clearance, $V_{1-\text{MERO}}$ and eGFR-MS were significantly decreased in cases versus controls, with higher variability of eGFR-MS in cases.

Conclusion Wide variation in meropenem concentrations in children with sepsis as compared to those without sepsis prompt close monitoring of GFR and drug concentrations in this population.

✉ Jennifer Le
jel078@health.ucsd.edu

✉ John S. Bradley
jbradley@rchsd.org

¹ University of California San Diego Skaggs School of Pharmacy and Pharmaceutical Sciences, La Jolla, CA, USA

² University of California Riverside, Riverside, CA, USA

³ San Diego School of Medicine, University of California, La Jolla, CA, USA

⁴ Rady Children's Hospital, San Diego, CA, USA

⁵ College of Pharmacy, University of Nebraska Medical Center, Omaha, NE, USA

⁶ Division of Biomedical Informatics, Omaha, USA

⁷ University of California, San Diego Health, La Jolla, CA, USA

Key Points

Adequate meropenem therapeutic exposure in critically ill children with sepsis is challenging due to variability of renal function that may change daily.

Prompt close monitoring of renal function and meropenem concentrations to refine dosing is essential for antibiotic efficacy and safety.

1 Background

Children admitted to the pediatric intensive care unit (PICU) with sepsis and septic shock are at risk for death and complications from the underlying infection and shock. Recently, multiple studies in adults with septic shock reported hyperfiltration of the kidneys at supra-physiologic rates (termed as augmented renal clearance, ARC) which subsequently raised great concerns for the inadequacy of standard drug dosing to treat these patients [1–3]. Limited population-based pharmacokinetic (PK) studies of commonly used antibiotics have demonstrated that the occurrence of ARC in critically ill children, ranges from 12% to as high as 67% using estimation of glomerular filtration rate (eGFR) [4–8]. The consequential aftermath of ARC in children suggests undertreatment of many of our sickest patients [6].

In addition to ARC, children in sepsis and septic shock may also experience acute kidney injury (AKI) during their PICU clinical course [9–11]. Both ARC and AKI alter kidney function, in which eGFR, calculated based on serum creatinine (SCr), is inaccurate in critically ill patients due to their fluctuating hemodynamic and renal perfusion status [12, 13]. The estimation of renal function using eGFR is inaccurate in AKI and ARC due to fluctuating SCr values that timely reflect renal function, particularly in those with anuria in AKI or fluid-overloaded in the ARC, which frequently occurs in critically ill children. In this study using a prospective cohort design, we aimed to evaluate the spectrum of renal function, from ARC to AKI, in critically ill infants and children with sepsis using meropenem PK and different eGFR assessments that integrate SCr and serum cystatin C (SCys) [5, 8]. Evaluation of the meropenem PK, specifically clearance (CL_{MERO}) and volume of distribution ($V_{\text{I-MERO}}$), will help inform dosing recommendations to achieve therapeutic and safe drug exposure in this vulnerable population with a spectrum of renal function, from ARC to AKI.

2 Methods

Using prospective design, we identified and enrolled infants (aged ≥ 4 weeks) and children (aged < 21 years) who were admitted from March 2019 to January 2023 to the PICU for at least 72 h with sepsis and/or septic shock as defined by the admission diagnosis by the attending physician, with the use of vasopressor therapy for shock; and treated with intravenous (IV) meropenem 20 mg/kg/dose every 8 h over 30 minutes as standard-of-care (maximum of 2000 mg/dose). These case participants were

matched to controls who were receiving meropenem as standard-of-care for other approved indications such as appendicitis, but did not demonstrate clinical findings of sepsis or hypotension. The protocol was approved by the University of California San Diego Institutional Review Board for Rady Children's Hospital (Project #181319, July 23, 2018).

Clinical and laboratory assessment was conducted daily from Days 1 to 7 of study enrollment; intensive sampling of serum meropenem concentrations and renal biomarkers: serum creatinine (SCr), serum cystatin C (SCys), and serum neutrophil gelatinase-associated lipocalin (SNGal) were assessed over 8 hours following administration of meropenem, on Days 1 to 3 for cases and on Day 1 for controls. Blood (0.25 mL) was collected at: pre-dose, 0.5-, 1-, 2-, 4-, and 8-h from the start of infusion for the first dose studied; and, pre-dose, 1-, 2-, 4-, 8-h with dosing on the 2 subsequent PICU days starting 24-h and 48-h after the initial dose studied. Sampled blood was immediately placed on ice, and centrifuged within 30 minutes, with plasma frozen at minus 70 °C prior to assay. Data extraction from charts included demographics; comorbid conditions (renal, blood infusion, Pediatric Logistic Organ Dysfunction [PELOD] score, diagnosis, pathogen); medications (antibiotics, diuretics, vasopressors; laboratory data [serum C-reactive protein, albumin, lactate]); and renal function (biomarkers, fluid balance). Pertinent data were extracted from the EPIC electronic health record software (Verona, WI) via Research Electronic Data Capture (REDCap, Vanderbilt University, Nashville, TN).

Due to the time-varying nature of some laboratory data (including renal biomarkers) that were necessary for population-based pharmacokinetic (pop-PK) analysis, a carry forward or backward method for the value nearest to the time for missing data was applied. For lactic acid and albumin, age-specific mean values were used when not available due to lack of clinical suspicion for abnormality as part of routine care.

2.1 Meropenem and Renal Biomarker Assays

Quantitative determination of meropenem was accomplished by liquid chromatography multiple reaction monitoring mass spectrometry (LC-MRM-MS) on an AB Sciex API 4000 LC-MS System. Multiple reaction monitoring (MRM) transition ion monitoring was performed in positive electrospray ionization mode with meropenem-d6 as an internal standard. Calibration standards were prepared in human plasma and used to generate an external 7-point calibration curve (313–20,000 ng/mL) using linear regression (1/ \times weighting) to plot the peak area ratio versus concentration. The calibration curves were linear ($R^2 \geq 0.99$) over the analytically measurable range.

Serum and urine creatinine were determined using the validated LC-MS/MS method [14]. In brief, 5–50 μL of sample were deproteinated and diluted with heavy isotope-labeled internal standard (ISTD) in a single step by adding ISTD in 80% acetonitrile. Twenty microliters of diluted sample were subjected to isocratic, HILIC HPLC with 10 mM ammonium acetate in 65% acetonitrile @ 0.15 mL/min. Creatinine and d3-creatinine ISTD were detected by electrospray ionization tandem mass spectrometry MRM transitions $114 > 44$ and $117 > 47$, respectively. Quantitation is achieved by comparing results to a synthetic standard calibration curve (0, 0.4, 1, 4, 10, 40 mmol/L for urine and 0, 0.2, 1, 5, 100 $\mu\text{g/mL}$ for serum).

Concentrations of SCys and SNgal were measured using enzyme-linked immunosorbent assay (ELISA) kit (LS Bio, catalog LS-F436 and LS-F10094, respectively) for the quantitative detection of cystatin C and Ngal, respectively, in samples of plasma, serum, and urine. For cystatin C, it is based upon a Sandwich assay principle with a detection range of 312–200,000 pg/mL and sensitivity < 312 pg/mL, with intra-assay CV < 10% and inter-assay CV < 12%. For Ngal, Sandwich assay principle was also applied, which detected levels as low as 3.9 pg/mL with intra-assay CV < 8% and inter-assay CV < 10%.

2.2 Renal Function Assessment

Renal function was assessed using different equations that incorporated SCr and SCys. The SCr values were evaluated by clinical and research assays; and SCys by research assay as described above. For SCr, the modified Schwartz and CKD-EPI formulae were used to calculate eGFR in children aged < 18 and ≥ 18 years, respectively (Online Resource 1) [12, 13]. The age- and sex-dependent Pierce equations were also used to determine eGFR using SCr and SCys [15]. Serum neutrophil gelatinase-associated lipocalin was screened as a covariate in the pop-PK modeling [16]. Based on published literature in pediatrics, the thresholds for ARC and AKI were >160 and ≥ 60 mL/min/1.73 m^2 , respectively (Online Resource 2).

2.3 Pharmacokinetic Modeling

We conducted pop-PK modeling of meropenem to characterize the variability in renal function from ARC to AKI. To handle the nonlinearity in the time-varying nature of meropenem's volume of distribution (V_1 and V_2) and clearance (CL_{MERO}), which were expected in our critically ill dynamic patients, pop-PK models were explored by non-linear mixed effects modeling using NONMEM 7.3 (Icon, Dublin, Ireland) with Pirana Workbench (Certara, Princeton, NJ) [17]. One-, two-, and three-compartment models with first-order elimination were tested

using ADVAN TRANS functions [18]. The First Order Conditional Estimation method was used with ETA-EPS interaction [19]. Proportional and additive residual error models were explored. To account for the expected variability in size of the participants, both V_{MERO} and CL_{MERO} were normalized to body weight (with allometric scaling of 0.75 for CL_{MERO} and isometric for V_{MERO}) in the base pop-PK model before evaluation of potential covariates [20, 21]. The elimination rate constant (k_e) was calculated by $\text{CL}/V_{1-\text{MERO}}$ and half-life by $0.693/k_e$.

The derivation of the final pop-PK was performed in a stepwise fashion with: (1) formulation of base PK model normalized to body weight; (2) Perl-speaks-NONMEM 5.3.0 was used to perform univariable and multivariable analyses. For univariable analysis, covariates that improved the model fit using a likelihood ratio test on the differences in the objective function of 4 ($p \leq 0.05$ for 1 degree of freedom) were selected for multivariate analysis. A forward selection (objective function reduction of 4, p value ≤ 0.05) and backward elimination (objective function reduction of 8, p value ≤ 0.005) were used in the multivariable analysis; (3) inspection of graphical data using goodness-of-fit diagnostic plots to assess the appropriateness of the structure for the base, intermediate and final models; (4) final pop-PK model selection with generation of empirical Bayesian estimates of individual subject PK parameters; and (5) assessment of parameter reliability using the bootstrap technique of 1000 to calculate the 95% confidence intervals (CI) for the population estimates [22]. In Perl-speaks-NONMEM, we employed valid states (or parameter-covariate parameterizations) of none, linear, exponential and power for continuous covariates, and none and linear for categorical covariates. For bootstrap, the model was considered reliable if the parameter estimates were within the 95% CI.

2.4 Statistical Analysis

We conducted statistical analyses using the post hoc dataset from the final pop-PK model that contained Bayesian estimates for both V_{MERO} and CL_{MERO} for each patient's entire duration of therapy. Study participants were divided into two groups (controls and cases), and compared by demographic, laboratory and PK data. For continuous variables, descriptive statistics included number of observations, mean, standard deviation (SD), median, minimum, maximum, and range values. Discrete-variable summaries included counts and proportions. All data and statistical tests were performed using appropriate tests (e.g., t-test for continuous and Chi-square for categorical variables) with two-tailed analyses using R version 4.3.0 (R-project.org, R Foundation for Statistical Computing, Vienna, Austria).

3 Results

We recruited and analyzed 27 children (19 cases and 8 controls) with median age of 11.8 (range 0.6–19.6) years and median weight 36.3 (range 7.2–98.0) kg. Of 309 observed meropenem serum concentrations, 271 were from cases (101–120) and the remaining 38 controls (201–212; Online Resource 5). Demographic data and baseline clinical characteristics were not significantly different between cases and controls, except for vasopressor use, fluid balance, PELOD score, c-reactive protein, serum albumin, and appendicitis (Table 1). In fact, most (88%)

controls had appendicitis, but they were not in shock and did not have sepsis. In addition, all serum biomarkers, including SCr, SCys, and SNGal, were significantly different between case and control groups (Online Resource 3). The quartile ranges for meropenem PK parameters and renal biomarkers are provided in Online Resource 3 for case and control subjects.

A 2-compartment (2-CMT) model, as compared with 1-CMT, significantly improved the fit of data by –33 change in objective function value (OFV). As anticipated, the inclusion of normalized weight on V_{1-MERO} and V_{2-MERO} , and normalized allometric weight on CL_{MERO} and Q_{MERO} significantly improved model fit, with change in OFC by –56.

Table 1 Baseline clinical characteristics^a

Clinical characteristic	Total <i>N</i> = 27	Control <i>n</i> = 8	Case <i>n</i> = 19	<i>p</i> -value
Age, y	11.8 (0.6–19.6)	10.2 (1.9–14.7)	14.2 (0.6–19.6)	0.9
4 wk to <6, <i>n</i> (%)	11 (41)	2 (25)	9 (47)	
6 wk to <12, <i>n</i> (%)	3 (11)	3 (38)	0 (0)	
≥ 12 wk, <i>n</i> (%)	13 (48)	3 (37)	10 (53)	
Male sex, <i>n</i> (%)	18 (67)	5 (63)	13 (68)	0.9
Weight, kg	36.3 (7.2–98.0)	42.4 (10.0–66.1)	36.3 (7.2–98.0)	0.7
Body surface area ^b m ²	1.18 (0.37–2.15)	1.26 (0.50–1.78)	1.18 (0.37–2.15)	0.7
Lean body mass ^b kg/m ²	27.24 (5.72–60.11)	30.23 (8.45–47.07)	27.24 (5.72–60.11)	0.8
Race/ethnicity				0.9
Hispanic	20 (74)	6 (75)	14 (74)	
Caucasian	19 (70)	4 (50)	15 (79)	
African-American	0 (0)	0 (0)	0 (0)	
Asian	0 (0)	0 (0)	0 (0)	
Other/unknown	8 (30)	4 (50)	4 (21)	
Vasopressor use, <i>n</i> (%)	11 (41)	0 (0)	11 (58)	0.02
Diuretic use, <i>n</i> (%)	1 (4)	0 (0)	1 (5)	0.8
Blood transfusion, <i>n</i> (%)	4 (15)	0 (0)	4 (21)	0.3
Appendicitis, <i>n</i> (%)	8 (30)	7 (88)	1 (5)	< 0.001
Fluid balance, mL/kg/24 h ^b	0.29 (–12.1 to 17.8)	2.31 (–2.4 to 6.2)	0.28 (–12.1 to 17.8)	0.02
Pediatric logistic organ dysfunction (PELOD) score	2 (0–11)	0 (0–0)	6 (0–11)	< 0.001
C-Reactive protein, mg/L				
Highest value	7.4 (0.1–35.3)	0.1 (0.1–2.8)	26.1 (1.5–35.3)	< 0.001
Serum albumin, g/dL				
Highest value	2.8 (2.1–4.3)	4.3 (3.8–4.3)	2.8 (2.2–3.5)	< 0.001
Lowest value	2.8 (2.1–4.3)	4.3 (3.8–4.3)	2.6 (2.1–3.5)	< 0.001
Serum bicarbonate, mEq/L				
Highest value	25.0 (18.0–43.0)	24.3 (22.0–26.0)	25.0 (18.0–43.0)	0.3
Lowest value	22.5 (18.0–38.0)	24.3 (22.0–26.0)	22.0 (18.0–38.0)	0.7
Serum lactate, mg/dL				
Highest value	1.4 (1.1–15.5)	1.4 (1.4–1.4)	1.6 (1.1–15.5)	0.07

^aNumbers represent median (range) unless otherwise stated

^bEquations for body surface area = (height [m] × weight [kg])/3600; lean body mass = 3.5 × (0.0215 × W^{0.6469} × H^{0.7236}) + 2; weight in kg and height in cm; and fluid balance = input – output (mL/kg/24 h)

Using a 2-CMT model with normalized weight, 42 intermediate models were created to characterize the meropenem PK parameters of $V_{1\text{-MERO}}$ and CL_{MERO} (Online Resource 4). Based on a univariate forward covariate screening, eGFR by the modified Schwartz and Pierce methods, presence of complicated appendicitis, and renal biomarkers were strong covariates for the PK parameters. The SCr measurements evaluated by both clinical and research assays produced comparable results in our pop-PK modeling. In addition, serum albumin (particularly its low value) was a significant covariate for $V_{1\text{-MERO}}$. After stepwise covariate modeling and selecting the model with the lowest OFV, the final PK model incorporated allometric weight and eGFR-MS as covariates for CL_{MERO} , and weight for V_{MERO} and also SCys on $V_{1\text{-MERO}}$ (Table 2). The inter-subject variability for $V_{1\text{-MERO}}$ and $V_{2\text{-MERO}}$ was assumed to be equal to prevent overfitting.

For the final model, scatterplots demonstrated good fit between observed and predicted population and individual concentrations (Fig. 1A). The conditional weighted residuals (CWRES), which were calculated based on the FOCE method, demonstrated that higher observed concentrations were under-predicted by the final model (Fig. 1B). The post hoc Bayesian population estimates for V_{MERO} and CL_{MERO} were similar to the median bootstrap analysis values, and were within the 95% CIs obtained from the bootstrap

analysis (Table 2). While V_{MERO} was statistically different, with decreased median V_{MERO} for cases, the range of $V_{1\text{-MERO}}$ for cases was wider demonstrating the significant variability in meropenem distribution in children with sepsis (Online Resource 3). Similarly, CL_{MERO} was significantly lower in cases than in controls.

4 Discussion

Meropenem's PK profile was best described by a 2-compartment model with first-order elimination, similar to previously published studies in both pediatrics and adults [23–28]. To our knowledge, this is the first study to assess renal biomarkers, specifically SCys and SNGal, in a popPK model of meropenem in children. Serum cystatin C is an extracellular biomarker that is not secreted nor reabsorbed by the kidney, making it an ideal biomarker for eGFR. Serum cystatin C, when adjusted for BSA, may be a more accurate way to determine eGFR compared to SCr in pediatric patients [29]. Serum cystatin C has also been used to predict AKI in pediatric patients with decompensated cirrhosis [30]. While SCys was an important covariate for CL_{MERO} in univariable analysis, it unexpectedly became a significant covariate for $V_{1\text{-MERO}}$ (central compartment) in our final PK model. As SCys is an extracellular biomarker, this may reflect fluid variability in our cohort to thereby impact $V_{1\text{-MERO}}$. The impact of SCys on meropenem's Vd should be further explored.

In hospitalized infants and children, the $V_{1\text{-MERO}}$ and CL_{MERO} were previously reported to range from 0.235 to 0.57 L/kg and 0.33 to 0.55 L/h/kg, respectively [23, 28, 31]. Previously published $V_{1\text{-MERO}}$ and CL_{MERO} were similar to our control non-septic participants (i.e., 0.29 L/kg and 0.29 L/h/kg, respectively). However, our compartmental popPK analysis showed decreased $V_{1\text{-MERO}}$ and CL_{MERO} for septic children (i.e., cases, 0.19 L/kg and 0.14 L/h/kg, respectively). The difference between the CL_{MERO} in our study and previous studies is likely due to the extreme variability of kidney function in our cohort, evident by a wide range of 0.05 to 0.39 L/kg/h (up to 8 times difference). Furthermore, the population evaluated in other studies was non-septic, clinically stable, received continuous renal replacement therapy or extracorporeal membrane oxygenation, or small sample size with limited age range; unlike our critically ill children with sepsis with elevated PELOD, CRP and vasopressor use [23, 27, 31]. Physiological changes in septic patients can cause profound changes in their hemodynamic status and renal function. In particular, sepsis can lead to changes in renal perfusion and has been associated with decreased (AKI) or increased (ARC) clearance for renally eliminated drugs, like meropenem.

Table 2 Final population-based pharmacokinetic model with bootstrap results^a

Parameter	Estimate	SE of estimate	Median bootstrap estimate	95% CI bootstrap
θ_{V1}	9.74	3.90	9.57	5.07–15.22
$\theta_{V1\text{-SCys}}$	0.449	0.428	0.421	0.113–1.63
θ_{V2}	4.53	1.23	4.45	2.78–6.53
θ_{CL}	9.72	2.37	9.78	7.23–13.16
$\theta_{CL\text{-eGFR-MS}}$	0.169	0.0967	0.195	0.105–0.514
θ_Q	1.66	0.400	1.61	0.84–3.89
η_{V1}, η_{V2}	0.306	0.0739	0.287	0.153–0.464
η_{CL}	0.487	0.103	0.483	0.286–0.687
ε	0.133	0.0205	0.127	0.093–0.173

CI confidence interval, CL clearance in L/h, SE standard error, V volume of distribution (1 = central compartment; 2 = peripheral compartment) in L; $\eta_{X=}$ intersubject random effect associated with V1, V2 or CL as denoted in subscript; ε = residual random effect, Wt weight in kg; eGFR-MS by Modified Schwartz = estimated glomerular filtration rate in mL/min/1.73 m²; and SCys = serum cystatin in ng/mL

^aFinal pharmacokinetic model was:

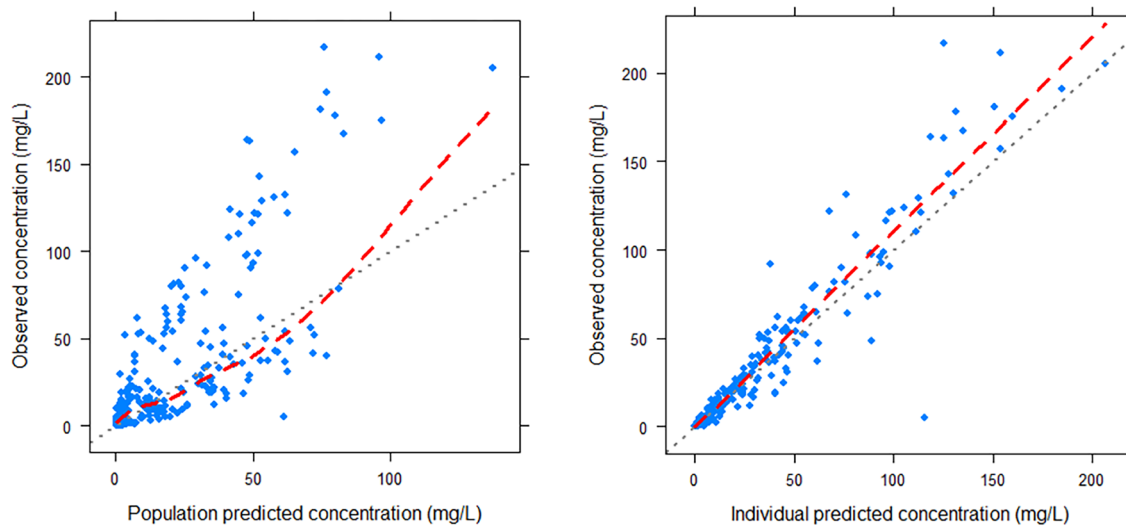
$$V1 (L) = \theta_{V1} * (Wt/70) * (1 + \theta_{V1\text{-SCys}} * SCys/0.45)$$

$$V2 (L) = \theta_{V2} * (Wt/70)$$

$$CL (L/h) = \theta_{CL} * (Wt/70)^{0.75} * [eGFR/140]^{\theta_{CL\text{-eGFR-MS}}}$$

$$Q (L/h) = \theta_Q * (Wt/70)^{0.75}$$

a) Observed versus Predicted Concentrations



b) Conditional Weighted Residuals

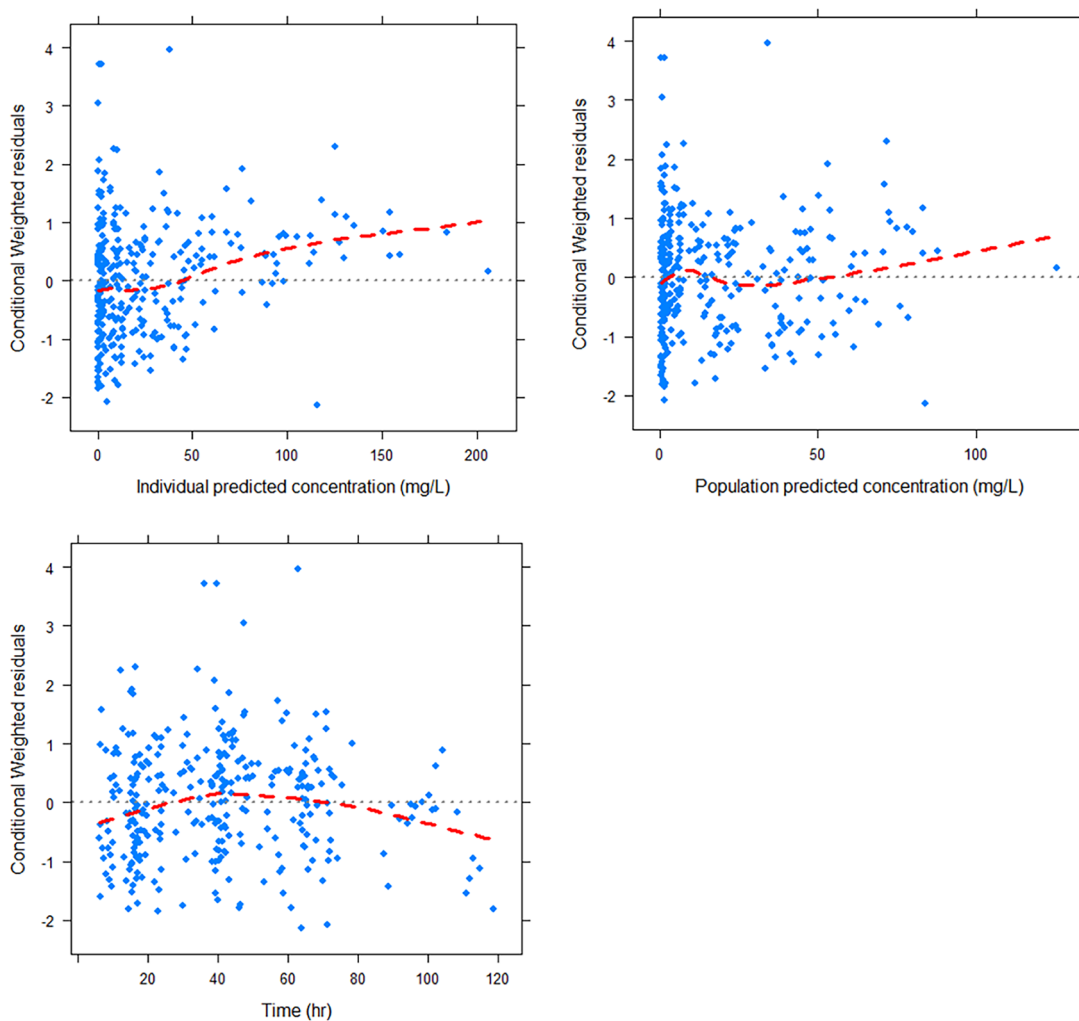


Fig. 1 Goodness-of-fit plots for the final meropenem population-based pharmacokinetic model, showing: observed concentrations versus population and individual predicted concentrations (a); and conditional weighted residuals versus individual predicted concentration, population predicted concentration, and time, respectively; (b) with the dashed line representing the line of identity or unity and the solid line representing the local regression smooth line (loess curve) Time refers to time after dose

Similarly, we observed decreased V_{1-MERO} in our cohort of septic children as compared to other studies, with minimal effect on the half-life due to consistent magnitude of change in both V_{1-MERO} and CL_{MERO} [23, 27, 31]. This difference in V_{1-MERO} is likely contributed by age, with older children in our cohort compared to those studied by Blumer (i.e., aged < 1 to 19 years vs 2 months to 12 years, respectively) and younger age in the studies by Cies et al (mean age, 3.1 ± 2.9 years) and Saito (median 1.4 [range 0.03–14.6] years) [23, 31]. Drug distribution alters with age, resulting from changes in body composition [32]. Furthermore, as a hydrophilic antibiotic, the V_{MERO} is affected by total body water content and the flow of extracellular fluids [33].

As meropenem is a renally eliminated drug, AKI has been associated with lower CL_{MERO} and ARC, to increased CL_{MERO} [34, 35]. In our study, CL_{MERO} was correlated with renal function using eGFR-MS that served as a covariate in our final PK model. In fact, there was a wide range of eGFR-MS in our study population. Patients with ARC were classified as those with eGFR-MS values exceeding 160 mL/min/1.73 m² [7, 36, 37]. Our cohort demonstrated a wide range of eGFR values, from 22.9 to 364.8 mL/min/1.73 m², with almost half with ARC by our definition. Limitations exist in the accuracy of calculation of eGFR with values above 200 mL/min/1.73 m², which are physiologically improbable. Acute decreases in SCr from fluid status may explain the exaggerated eGFR values in some cases.

While we attempted to identify ARC in children with sepsis, we did not collect urine to compare to our eGFR estimations. However, our research group has previously published studies on pediatric ARC and identified thresholds of 130 mL/min/1.73 m² using vancomycin and aminoglycoside clearance, and 160 mL/min/1.73 using eGFR by modified Schwartz [5, 7, 38].

With the significant PK variation in both V_{MERO} and CL_{MERO} in septic children, the daily dose of meropenem is expected to change accordingly. Augmented renal clearance can lead to subtherapeutic antimicrobial exposure as meropenem is cleared rapidly, which has been documented for meropenem in critically ill children [27]. This leads to poor target attainment when targeting time above minimum inhibitory concentration ($T > MIC$), particularly for therapeutic goals of 70% and 100% $T > MIC$ for patients with sepsis. In our cohort, the variability in V_{MERO} was also notable and should not be ignored for evaluation in septic children since

V_{MERO} also impacts dose, especially important early in the therapeutic course to optimize drug exposure for the initial effective management of sepsis. Future studies with large sample size should investigate the impact of the PK variability of both V_{MERO} and CL_{MERO} on meropenem dosing in critically ill children using Monte Carlo simulation since higher doses, even incorporating prolonged or continuous infusion, may be needed as reported in children and adults with severe sepsis and septic shock, which is particularly prudent when treating pathogens with high MIC > 4 µg/mL [27, 39–41]. Future studies should also include children with diverse comorbidities and polypharmacy inclusive of those with synergistic risks for renal impairment.

There were several limitations in our study. First, we designed a prospective study to enhance our understanding of PK alterations in septic children, compared to those without sepsis to determine the spectrum of renal function. To maximize sample collection as part of routine care, blood collection of children without sepsis (i.e., controls) was confined to limited PK sampling and first day of study enrollment. In contrast, we measured concentrations more intensively in septic children and up to Day 3 of meropenem therapy. Therefore, our final PK model more reflects children with sepsis. However, even with the limited sampling strategy, coupled to the limited sample size of children without sepsis, differences in PK parameters were already observed.

5 Conclusion

Notable changes and wide variability in meropenem PK, including both V_{MERO} and CL_{MERO} , contribute to different drug exposure in critically ill children. Meropenem exposure may even change daily, necessitating the need to closely monitor renal function in critically ill children with anticipated hemodynamic changes. Due to these dynamic changes, future studies are crucial to evaluate, from a learning health system approach, the feasibility and outcomes in optimal meropenem monitoring inclusive of machine learning paired with current methods that are standard of care.

Supplementary Information The online version contains supplementary material available at <https://doi.org/10.1007/s40262-025-01495-3>.

Declarations

Funding This research was supported by Grant Number R01 HD095547 to J.S.B. from the Eunice Kennedy Shriver National Institute of Child Health and Human Development. The content is solely the responsibility of the authors and does not necessarily represent the official views of the Eunice Kennedy Shriver National Institute of Child Health and Human Development, or the National Institutes of Health.

Conflict of interest The authors have no competing interests relevant to this article to disclose.

Data availability The data that support the findings of this study are not openly available for reasons of sensitivity and risk of reidentification due to its clinical nature. Data, however, are available from the authors upon reasonable request.

Ethics approval The protocol for this study was approved by the University of California San Diego Institutional Review Board for Rady Children's Hospital (Project #181319, July 23, 2018).

Consent to participate Informed consent to participate in the study was obtained from all participants or their legal guardians.

Consent for publication All participants provided informed consent for the publication of their data.

Code availability Not applicable.

Authors' contribution John Bradley and Jennifer Le contributed to designing and performing the study. Data collection and analysis was performed by John Bradley, Jennifer Le, Julie Huynh, Brandon Vo, Annie Mai, Robert Mak, Jeremiah Momper, Edmund Caparelli, Helen Harvey, and Sean Avedissian. The draft of the manuscript was written by John Bradley, Jennifer Le, Julie Huynh, Brandon Vo, Annie Mai, Erin Bradley, Amy Sitapati, and Karandeep Singh and all authors reviewed and commented on previous versions of the manuscript. All authors read and approved the final manuscript.

Open Access This article is licensed under a Creative Commons Attribution-NonCommercial 4.0 International License, which permits any non-commercial use, sharing, adaptation, distribution and reproduction in any medium or format, as long as you give appropriate credit to the original author(s) and the source, provide a link to the Creative Commons licence, and indicate if changes were made. The images or other third party material in this article are included in the article's Creative Commons licence, unless indicated otherwise in a credit line to the material. If material is not included in the article's Creative Commons licence and your intended use is not permitted by statutory regulation or exceeds the permitted use, you will need to obtain permission directly from the copyright holder. To view a copy of this licence, visit <http://creativecommons.org/licenses/by-nc/4.0/>.

References

1. Udy AA, De Waele JJ, Lipman J. Augmented renal clearance and therapeutic monitoring of β -lactams. *Int J Antimicrob Agents*. 2015;45(4):331–3. <https://doi.org/10.1016/j.ijantimicag.2014.12.020>.
2. Hefny F, Stuart A, Kung JY, Mahmoud SH. Prevalence and risk factors of augmented renal clearance: a systematic review and meta-analysis. *Pharmaceutics*. 2022. <https://doi.org/10.3390/pharmaceutics14020445>.
3. Cook AM, Hatton-Kolpek J. Augmented renal clearance. *Pharmacotherapy*. 2019;39(3):346–54. <https://doi.org/10.1002/phar.2231>.
4. Van Der Heggen T, Dhont E, Peperstraete H, et al. Augmented renal clearance: a common condition in critically ill children. *Pediatr Nephrol*. Jun2019;34(6):1099–106. <https://doi.org/10.1007/s00467-019-04205-x>.
5. Avedissian SN, Bradley E, Zhang D, et al. Augmented renal clearance using population-based pharmacokinetic modeling in critically ill pediatric patients. *Pediatr Crit Care Med*. 2017;18(9):e388–94. <https://doi.org/10.1097/pcc.0000000000001228>.
6. Dhont E, Van Der Heggen T, De Jaeger A, Vande Walle J, De Paep P, De Cock PA. Augmented renal clearance in pediatric intensive care: are we undertreating our sickest patients? *Pediatr Nephrol*. 2020;35(1):25–39. <https://doi.org/10.1007/s00467-018-4120-2>.
7. Avedissian SN, Skochko SM, Le J, et al. Use of simulation strategies to predict subtherapeutic meropenem exposure caused by augmented renal clearance in critically ill pediatric patients with sepsis. *J Pediatr Pharmacol Ther*. 2020;25(5):413–22. <https://doi.org/10.5863/1551-6776-25.5.413>.
8. Avedissian SN, Rhodes NJ, Kim Y, Bradley J, Valdez JL, Le J. Augmented renal clearance of aminoglycosides using population-based pharmacokinetic modelling with Bayesian estimation in the paediatric ICU. *J Antimicrob Chemother*. 2020;75(1):162–9. <https://doi.org/10.1093/jac/dkz408>.
9. Kaddourah A, Basu RK, Bagshaw SM, Goldstein SL. Epidemiology of acute kidney injury in critically ill children and young adults. *N Engl J Med*. 2017;376(1):11–20. <https://doi.org/10.1056/NEJMoa1611391>.
10. Formeck CL, Joyce EL, Fuhrman DY, Kellum JA. Association of acute kidney injury with subsequent sepsis in critically ill children. *Pediatr Crit Care Med*. 2021;22(1):e58–66. <https://doi.org/10.1097/pcc.0000000000002541>.
11. Alobaidi R, Anton N, Burkholder S, et al. Association between acute kidney injury duration and outcomes in critically ill children. *Pediatr Crit Care Med*. 2021;22(7):642–50. <https://doi.org/10.1097/pcc.0000000000002679>.
12. Inker LA, Eneanya ND, Coresh J, et al. New creatinine- and cystatin c-based equations to estimate GFR without race. *N Engl J Med*. 2021;385(19):1737–49. <https://doi.org/10.1056/NEJMoA2102953>.
13. Schwartz GJ, Work DF. Measurement and estimation of GFR in children and adolescents. *Clin J Am Soc Nephrol*. 2009;4(11):1832–43. <https://doi.org/10.2215/cjn.01640309>.
14. Young S, Struys E, Wood T. Quantification of creatine and guanidinoacetate using GC-MS and LC-MS/MS for the detection of cerebral creatine deficiency syndromes. *Curr Protoc Hum Genet*. 2007;Chapter 17:Unit 17.3. <https://doi.org/10.1002/0471142905.hg1703s54>.
15. Pierce CB, Muñoz A, Ng DK, Warady BA, Furth SL, Schwartz GJ. Age- and sex-dependent clinical equations to estimate glomerular filtration rates in children and young adults with chronic kidney disease. *Kidney Int*. 2021;99(4):948–56. <https://doi.org/10.1016/j.kint.2020.10.047>.
16. Wheeler DS, Devarajan P, Ma Q, et al. Serum neutrophil gelatinase-associated lipocalin (NGAL) as a marker of acute kidney injury in critically ill children with septic shock. *Crit Care Med*. 2008;36(4):1297–303. <https://doi.org/10.1097/CCM.0b013e318169245a>.
17. Beal S, Boeckmann L, Bauer R, Sheiner L. NONMEM user's guides. (1989–2009). 2009.
18. Bradley JS, Sauberman JB, Ambrose PG, Bhavnani SM, Rasmussen MR, Capparelli EV. Meropenem pharmacokinetics, pharmacodynamics, and Monte Carlo simulation in the neonate. *Pediatr Infect Dis J*. 2008;27(9):794–9. <https://doi.org/10.1097/INF.0b013e318170f8d2>.
19. Bauer RJ. NONMEM tutorial part II: estimation methods and advanced examples. *CPT Pharmacomet Syst Pharmacol*. 2019;8(8):538–56. <https://doi.org/10.1002/psp4.12422>.
20. Le J, Bradley JS. Optimizing antibiotic drug therapy in pediatrics: current state and future needs. *J Clin Pharmacol*. 2018;58(Suppl 10):S108–s122. <https://doi.org/10.1002/jcph.1128>.
21. Anderson BJ, Allegaert K, Holford NH. Population clinical pharmacology of children: modelling covariate effects.

- Eur J Pediatr. 2006;165(12):819–29. <https://doi.org/10.1007/s00431-006-0189-x>.
22. Ette EI, Williams PJ, Lane JR. Population pharmacokinetics III: design, analysis, and application of population pharmacokinetic studies. *Ann Pharmacother*. 2004;38(12):2136–44. <https://doi.org/10.1345/aph.1E260>.
23. Cies JJ, Moore WS 2nd, Enache A, Chopra A. Population pharmacokinetics and pharmacodynamic target attainment of meropenem in critically ill young children. *J Pediatr Pharmacol Ther* Jul-Aug. 2017;22(4):276–85. <https://doi.org/10.5863/1551-6776-22.4.276>.
24. Ehmann L, Zoller M, Minichmayr IK, et al. Development of a dosing algorithm for meropenem in critically ill patients based on a population pharmacokinetic/pharmacodynamic analysis. *Int J Antimicrob Agents*. 2019;54(3):309–17. <https://doi.org/10.1016/j.ijantimicag.2019.06.016>.
25. Lan J, Wu Z, Wang X, et al. Population pharmacokinetics analysis and dosing simulations of meropenem in critically ill patients with pulmonary infection. *J Pharm Sci*. 2022;111(6):1833–42. <https://doi.org/10.1016/j.xphs.2022.01.015>.
26. Zhao Y-C, Zou Y, Xiao Y-W, et al. Does prolonged infusion time really improve the efficacy of meropenem therapy? A prospective study in critically ill patients. *Infect Dis Ther*. 2022;11(1):201–16. <https://doi.org/10.1007/s40121-021-00551-2>.
27. Saito J, Shoji K, Oho Y, et al. Population pharmacokinetics and pharmacodynamics of meropenem in critically ill pediatric patients. *Antimicrob Agents Chemother*. 2021. <https://doi.org/10.1128/AAC.01909-20>.
28. Morales Junior R, Mizuno T, Paice KM, et al. Identifying optimal dosing strategies for meropenem in the paediatric intensive care unit through modelling and simulation. *J Antimicrob Chemother*. 2024;79(10):2668–77. <https://doi.org/10.1093/jac/dkae274>.
29. Kilpatrick ES, Keevil BG, Addison GM. Does adjustment of GFR to extracellular fluid volume improve the clinical utility of cystatin C? *Arch Dis Child*. 2000;82(6):499–502. <https://doi.org/10.1136/adc.82.6.499>.
30. Vijay P, Lal BB, Sood V, Khanna R, Alam S. Cystatin C: best biomarker for acute kidney injury and estimation of glomerular filtration rate in childhood cirrhosis. *Eur J Pediatr*. 2021;180(11):3287–95. <https://doi.org/10.1007/s00431-021-04076-1>.
31. Blumer JL, Reed MD, Kearns GL, et al. Sequential, single-dose pharmacokinetic evaluation of meropenem in hospitalized infants and children. *Antimicrob Agents Chemother*. 1995;39(8):1721–5. <https://doi.org/10.1128/AAC.39.8.1721>.
32. Mangoni AA, Jackson SH. Age-related changes in pharmacokinetics and pharmacodynamics: basic principles and practical applications. *Br J Clin Pharmacol*. 2004;57(1):6–14. <https://doi.org/10.1046/j.1365-2125.2003.02007.x>.
33. Ruggiero A, Ariano A, Triarico S, Capozza MA, Ferrara P, Attina G. Neonatal pharmacology and clinical implications. *Drugs Context*. 2019;8: 212608. <https://doi.org/10.7573/dic.212608>.
34. Ehmann L, Zoller M, Minichmayr IK, et al. Role of renal function in risk assessment of target non-attainment after standard dosing of meropenem in critically ill patients: a prospective observational study. *Crit Care*. 2017;21(1):263. <https://doi.org/10.1186/s13054-017-1829-4>.
35. Gijssen M, Elkayal O, Annaert P, et al. Meropenem target attainment and population pharmacokinetics in critically ill septic patients with preserved or increased renal function. *Infect Drug Resist*. 2022;15:53–62. <https://doi.org/10.2147/IDR.S343264>.
36. He CY, Ye PP, Liu B, Song L, van den Anker J, Zhao W. Population pharmacokinetics and dosing optimization of vancomycin in infants, children, and adolescents with augmented renal clearance. *Antimicrob Agents Chemother*. 2021;65(10):e0089721. <https://doi.org/10.1128/AAC.00897-21>.
37. Hirai K, Ihara S, Kinae A, et al. Augmented renal clearance in pediatric patients with febrile neutropenia associated with vancomycin clearance. *Ther Drug Monit*. 2016;38(3):393–7. <https://doi.org/10.1097/FTD.0000000000000270>.
38. Avedissian SN, Rohani R, Bradley J, Le J, Rhodes NJ. Optimizing aminoglycoside dosing regimens for critically ill pediatric patients with augmented renal clearance: a convergence of parametric and nonparametric population approaches. *Antimicrob Agents Chemother*. 2021. <https://doi.org/10.1128/AAC.02629-20>.
39. Wang Y, Li H, Wang D, et al. Changes of PK/PD of Meropenem in patients with abdominal septic shock and exploration of clinical rational administration plan: a prospective exploratory study. *Sci Rep*. 2024;14(1):10173. <https://doi.org/10.1038/s41598-024-60909-7>.
40. Eisert A, Lanckohr C, Frey J, et al. Comparison of two empirical prolonged infusion dosing regimens for meropenem in patients with septic shock: a two-center pilot study. *Int J Antimicrob Agents*. 2021;57(3): 106289. <https://doi.org/10.1016/j.ijantimicag.2021.106289>.
41. Jaruratanasirikul S, Thengyai S, Wongpoowarak W, et al. Population pharmacokinetics and Monte Carlo dosing simulations of meropenem during the early phase of severe sepsis and septic shock in critically ill patients in intensive care units. *Antimicrob Agents Chemother*. 2015;59(6):2995–3001. <https://doi.org/10.1128/AAC.04166-14>.